Terahertz emission from (100) InAs surfaces at high excitation fluences

M. Reid and R. Fedosejevs[a)]
Department of Electrical Engineering, University of Alberta, Edmonton, Canada T6G 2V4

(Received 19 January 2004; accepted 29 October 2004; published online 23 December 2004)

The radiated terahertz field from (100) InAs surfaces under excitation at fluences of millijoules per centimeter squared has been studied in detail in order to identify the main generation mechanism. We find that the terahertz emission depends strongly on pump polarization, and that the predominant emission mechanism appears to be the surface nonlinear optical response of the InAs crystal. A saturation fluence of 29 ± 4 $\mu J/cm^2$ is found for the emission. © *2005 American Institute of Physics*. [DOI: 10.1063/1.1842863]

Techniques for generating radiation in the terahertz (THz) frequency band are of increasing interest today, due to a growing number of applications using such radiation. In the last two decades, THz radiation sources have been developed using ultrafast laser sources to excite photoconductive switches,[1] semiconductor surfaces,[2] and nonlinear processes in materials.[3,4]

Of the various THz emitters, InAs surface emission has received much attention after initial reports of high conversion efficiency.[5] Since this time, InAs has proven to be a relatively bright source of THz radiation when using low irradiance fluences ($\leqslant$100 nJ/cm^2), especially under the influence of a magnetic field.[6–8] Conversion efficiencies from InAs in the range of $\sim10^{-5}$ in this low fluence regime[7] are still significantly less than that of the best THz emitters reported to date ($\sim10^{-3}$) using large-aperture externally biased GaAs photoconductive switches.[9] Thus, it is of interest to study the increase and saturation of emitted radiation from InAs sources using higher irradiation fluences.

Traditionally, THz emission from InAs is reported to be a result of photoexcited carrier diffusion (photo-Dember effect).[10,11] For other wide-band-gap materials such as InP and GaAs,[12,13] there is evidence that optical rectification (OR) can contribute significantly to the generation of THz radiation, which has also been reported for narrow-band-gap materials such as InSb (Ref. 14) and (111) InAs (Ref. 15). Recently, it has been reported that there is a negligible contribution from OR in (100) InAs at low and moderate excitation fluences.[16–18] However, it is important to properly identify the emission mechanism in order to fully understand the scaling of emission to higher output fluences. In the present letter, we have studied the saturation of emission for (100) InAs and the polarization dependence of the THz emission in the saturated regime in order to clearly identify the generation mechanism.

A regeneratively amplified Ti:sapphire laser system generates 800 nm, 1 kHz, 750 μJ, 130 fs pulses. The radiation is split into a pump (92%) and probe (4%) using a wedged window. The probe is delayed with respect to the pump using an optical delay line. A variable attenuator ($\lambda/2$ plate and polarizer) is used in the pump beam to vary the fluence. The polarizer can be removed to allow the linear polarization angle of the pump to be modified. The THz radiation from the emitter is collected and imaged onto the detector using four $F/2$ parabolic mirrors. The probe is co-linearly propagated through a 1-mm-thick, (110) ZnTe electro-optic crystal, with the THz field. This induces a polarization modulation which is analyzed using a polarization bridge ($\lambda/4$ plate and Wollaston prism), with the differential photodiode signal detected using a lock-in amplifier at the optical chopping frequency of approximately 330 Hz. The orientation of the (001) axis of the ZnTe crystal is varied to measure the electro-optic signal from either *p*- or *s*-polarized generated THz field.[19] The InAs emitter is a (100)-oriented, undoped, *n*-type InAs sample illuminated at an incidence angle of 45° (conduction band carrier density and dc mobility are 1.9×10^{16} cm^{-3} and 2.5×10^4 cm^2 V^{-1} s^{-1}, respectively). The pump beam is telescoped to a $1/e^2$ intensity beam diameter of 2.9 ± 0.05 mm using a pair of lenses, and the emitted radiation is collected at an angle of 45° to the surface normal in the specular direction.

The crystallographic orientation of the InAs sample was rotated about the surface normal [100], while irradiating the sample with a linearly *p*-polarized pump beam at an excitation fluence of approximately 2 mJ/cm^2. As seen in Fig. 1, the *p*-polarized output consists of large constant component plus a small component with twofold rotational symmetry. The angularly independent component could be attributed to emission from the photo-Dember effect, which should lead to constant *p*-polarized output, independent of crystal rotation. It could also be attributed to a transient current resulting from the acceleration of photogenerated carriers in the surface depletion field. However, this contribution is small compared to the photo-Dember effect in InAs at low fluence.[16]

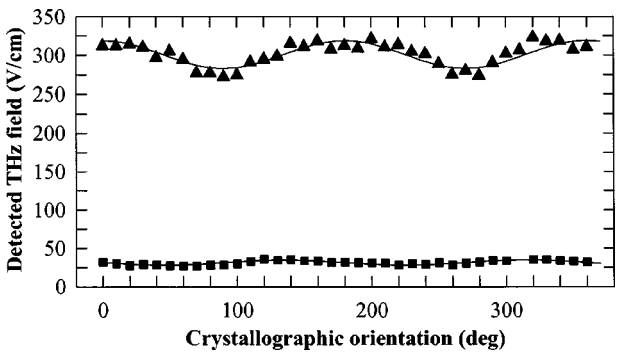

FIG. 1. *p*- (triangles) and *s*-polarized (squares) THz signals as a function of the crystallographic orientation for a *p*-polarized pump beam at approximately 2 mJ/cm^2. The angle in the plot is defined as the angle the *p*-polarized pump beam at the (100) face makes with the [011] direction.

[a)]Electronic mail: rfed@ee.ualberta.ca

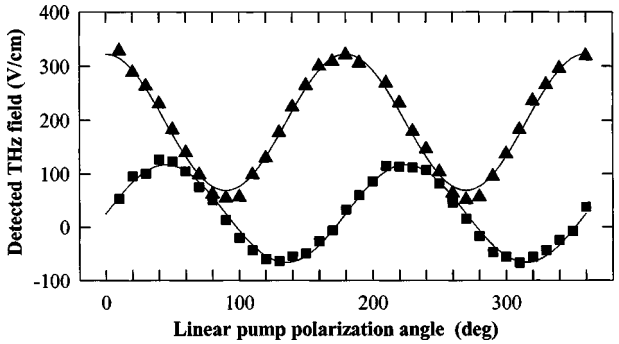

FIG. 2. Detected *p*- (triangles) and *s*-polarized (squares) THz field as a function of the linear pump polarization angle at 1.7 mJ/cm^2 pump fluence. 0° corresponds to a *p*-polarized pump beam while 90° corresponds to an *s*-polarized beam. The InAs crystal axes are such that the [011] axis is perpendicular to the plane of incidence.

We will refer to these as photocarrier-related effects. It is therefore tempting to attribute the emission to photocarrier-related effects. However, it will be shown that this is not the case.

The angle of the linearly polarized pump was also varied, while maintaining the InAs crystal fixed with the [011] axis perpendicular to the plane of incidence. The two polarizations of the THz signal were measured at a beam fluence of 1.7 mJ/cm^2 and plotted in Fig. 2. There is a very strong twofold rotational symmetry, both in the *s*- and *p*-polarized THz signals. A small part of the angular variation in the *p*-polarized THz signal can be due to variations in Fresnel reflectivity with input polarization since there is a difference in the transmission for *p*- and *s*-polarized radiation into the InAs ($T_p=0.81$ and $T_s=0.57$ for $n=3.5$ at 800 nm and 45° incidence angle). The variation in the *p*-polarized THz signal for the 0° orientation angle shown in Fig. 2 versus the pump beam fluence is plotted in Fig. 3. The data fits the saturation formula $E_{\mathrm{THz}}^{\mathrm{pk}}=(AF)/(F+F_{\mathrm{sat}})$, where A is the amplitude, F is the incident beam fluence and F_{sat} is the saturation fluence, with a best-fit saturation fluence of $F_{\mathrm{sat}}=29\pm4\ \mu J/cm^2$. Since the angular dependence shown in Fig. 2 was measured at an incident fluence of 1.7 mJ/cm^2, very little reduction in output would be expected for even a factor of 2 reduction of pump fluence, and thus only a very small part of the rotational anisotropy shown in Fig. 2 can be related to Fresnel reflection effects. In addition, it is not expected that a small change in Fresnel reflectivity at the pump wavelength from the injection of carriers by the laser at the present intensities will modify this conclusion significantly.

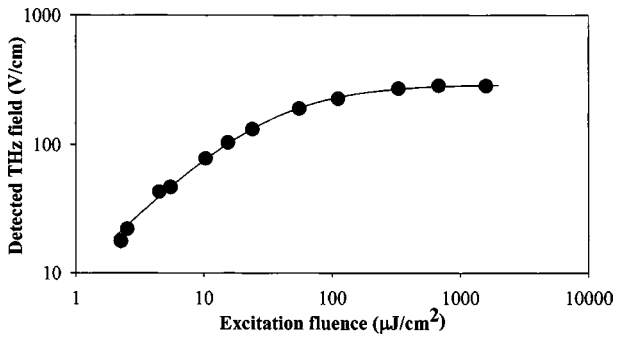

FIG. 3. Detected *p*-polarized THz field as a function of excitation fluence. The fluence is defined as the excitation fluence normal to beam propagation before striking the surface of the InAs crystal.

Since there can be no *s*-polarized emission from a dipole radiating normal to a dielectric discontinuity,[20] the *s*-polarized THz signal in Fig. 2 indicates that there is a significant nonlinear optical response. Another feature of results shown in Fig. 2 is that the radiated *s*-polarized THz field is 45° phase shifted from the *p*-polarized THz signal and exhibits phase reversal under polarization rotation.

The main features that must be explained by any mechanism responsible for the radiated THz field are: (i) large *p*-polarized isotropic signal under crystal rotation, (ii) large polarization dependence of *s*- and *p*-polarized THz signals under pump polarization rotation, (iii) 45° relative phase between the data sets of *p*- and *s*-polarized THz signals in Fig. 2, and (iv) change of polarity in *s*-polarized THz signal under pump polarization rotation. These can be described satisfactorily by the emission mechanism being surface OR. For the similar phenomenon of surface second-harmonic generation (SHG) from (100) facets of crystals with $\bar{4}3m$ symmetry, the *s*-polarized emitted field is proportional to $E_s^{\mathrm{pump}}E_p^{\mathrm{pump}}$, while the *p*-polarized emitted field is proportional to a linear combination of $(E_s^{\mathrm{pump}})^2$ and $(E_p^{\mathrm{pump}})^2$ [see Eq. (30) and Table IV of Ref. 21]. The constants of proportionality depend on the linear optical properties and surface nonlinear tensor elements of the InAs but *not* on the crystallographic orientation. The emission depends only on *pump polarization*, consistent with points (i) and (ii). The fact that there is a small nonzero *s*-polarized THz signal in Fig. 1 will be discussed later. The large *s*-polarized THz signal with a change in polarity and twofold rotational symmetry 45° out of phase with the data set for *p*-polarized THz radiation is simply described by $E_s^{\mathrm{THz}}\propto E_s^{\mathrm{pump}}E_p^{\mathrm{pump}}$, and E_p^{THz} having a large $(E_p)^2$ and small $(E_s)^2$ contribution [see Eq. (30) and Table IV of Ref. 21], consistent with points (iii) and (iv).

At this point, it is worth noting that there are other possible mechanisms that cannot be ruled out without discussion. These are electric-field-induced OR[12] (similar to electric-field-induced SHG[22]), bulk OR, and the quadrupolar nonlinear response of InAs.

Calculating the bulk contribution for our configuration, there is no angularly independent term for either crystal or pump polarization angle rotation.[22] The small signal modulating the large offset of the *p*-polarized THz signal of Fig. 1 would be consistent with *bulk* OR.

Electric-field-induced second-harmonic or optical rectification is a result of the near-surface depletion field mixing with the third-order susceptibility, resulting in an effective second-order response of the material.[12,22] The $\bar{4}3m$ and (100) orientation of the InAs dictate that the tensor elements describing the process of electric-field-induced effective second order nonlinearity are exactly in the same form as described by Ref. 21 for a pure surface response. The description in Ref. 21 is phenomenological in nature, and therefore encompasses the related process of the effective second order response due to the depletion field. It is therefore impossible to distinguish between the two processes with crystallographic orientation and polarization studies alone. We will refer to these two processes as the effective second-order surface response of InAs.

Finally, the quadrupolar response of the InAs could lead to a large isotropic contribution under crystal rotation as observed in Fig. 1. We rule out this possibility by noting that there is no fourfold symmetric contribution observable, and

the isotropic and crystallographic angular-dependent contributions from the quadrupolar nonlinearity are expected to be within a factor of 4 of each other in magnitude by calculating the contributions using the index of refraction of InAs and an angle of incidence of 45° [see Eq. (17) and Table II of Ref. 21].

We therefore conclude that the dominant emission mechanism at our reported fluences is the effective *surface* nonlinear optical response of InAs. This may also explain some recent results that report a reduced dependence of THz signal strength on magnetic field as the excitation fluence is increased,[18] since it is expected that the magnetic field predominantly affects the directionality of moving charges in the photocarrier-related mechanisms but has little effect on the nonlinear surface mechanisms. The residual offset in *s*-polarized THz signal seen in Figs. 1 and 2 cannot easily be explained by the mechanisms just discussed and is possibly due to higher order effects such as the photon-drag effect.[23]

The twofold rotational signal apparent under crystallographic rotation is likely due to *bulk* optical rectification. The relative contribution is estimated to be approximately 13% of the total signal. The offset observed for *p*-polarized THz signal in Fig. 2 is likely due to photocarrier related effects. Assuming negligible Fresnel coupling effects (emission is saturated), this contribution is approximately 20%. That the emission is reported to be a result of the photo-Dember effect at low excitation fluences[16,17] may indicate that the saturation fluences for the photocarrier related effects are substantially less than that for OR at the surface. More work is required to clearly identify the crossover from carrier-diffusion-dominated to surface-optical-rectification-dominated emission.

Financial support for the research provided by MPB Technologies, Inc., and the Natural Sciences and Engineering Research Council of Canada is gratefully acknowledged.

[1] D. Auston, K. Cheunk, and P. Smith, Appl. Phys. Lett. **45**, 284 (1984).
[2] X.-C. Zhang and D. H. Auston, J. Appl. Phys. **71**, 326 (1992).
[3] B. B. Hu, X.-C. Zhang, D. Auston, and P. Smith, Appl. Phys. Lett. **56**, 506 (1990).
[4] L. Xu, X.-C. Zhang, and D. Auston, Appl. Phys. Lett. **61**, 1784 (1992).
[5] N. Sarakura, H. Ohtake, S. Izumida, and Z. Liu, J. Appl. Phys. **84**, 654 (1998).
[6] C. Weiss, R. Wallenstein, and R. Beigang, Appl. Phys. Lett. **77**, 4160 (2000).
[7] R. Mclaughlin, A. Corchia, M. Johnston, Q. Chen, C. Ciesla, D. Arnone, G. Jones, E. Linfield, A. Davies, and M. Pepper, Appl. Phys. Lett. **76**, 2038 (2000).
[8] J. Heyman, P. Neocleous, D. Hevert, P. Crowell, T. Mueller, and K. Unterrainer, Phys. Rev. B **64**, 085202 (2001).
[9] D. You, P. H. Bucksbaum, and D. R. Dykaar, Opt. Lett. **18**, 290 (1993).
[10] T. Dekorsy, H. Auer, H. Bakker, H. Roskos, and H. Kurz, Phys. Rev. B **53**, 4005 (1996).
[11] M. B. Johnston, D. Whittaker, A. Corchia, A. Davies, and E. Linfield, Phys. Rev. B **65**, 165301 (2002).
[12] S. Chuang, S. Schmitt-Rink, B. Greene, P. Saeta, and A. Levi, Phys. Rev. Lett. **68**, 102 (1992).
[13] B. Greene, P. Saeta, D. Dykaar, S. Schmitt-Rink, and S. Chuang, IEEE J. Quantum Electron. **28**, 2302 (1992).
[14] S. C. Howells and L. A. Schlie, Appl. Phys. Lett. **67**, 3688 (1995).
[15] S. Kono, P. Gu, M. Tani, and K. Sakai, Appl. Phys. B: Lasers Opt. **71**, 901 (2000).
[16] P. Gu, M. Tani, S. Kono, K. Sakai, and X.-C. Zhang, J. Appl. Phys. **91**, 5533 (2002).
[17] H. Takashi, A. Quema, M. Goto, S. Ono, and N. Sarakura, Jpn. J. Appl. Phys., Part 1 **42**, L1259 (2003).
[18] H. Takahashi, A. Quema, R. Yoshioka, and N. Sarakura, Appl. Phys. Lett. **83**, 1068 (2003).
[19] P. C. M. Planken, H.-K. Nienhuys, H. Bakker, and T. Wenckebach, J. Opt. Soc. Am. B **18**, 313 (2001).
[20] W. Lukosz, J. Opt. Soc. Am. **69**, 1495 (1979).
[21] J. E. Sipe, D. Moss, and H. van Driel, Phys. Rev. B **35**, 1129 (1987).
[22] T. A. Germer, K. Kolasinski, J. Stephenson, and L. Richter, Phys. Rev. B **55**, 10694 (1997).
[23] I. M. Catalano and A. Cingolani, Solid State Commun. **37**, 183 (1981).